Estimating cooling capacities from aerial images using convolutional neural networks

Florian Barth [a,*], Simon Schüppler [b], Kathrin Menberg [a], Philipp Blum [a]

[a] Karlsruhe Institute of Technology (KIT), Institute of Applied Geosciences (AGW), Kaiserstraße 12, 76131 Karlsruhe, Germany

[b] European Institute for Energy Research (EIFER), Emmy-Noether-Strase 11, 76131 Karlsruhe, Germany

* Corresponding author: Florian Barth, Tel: +49 721 608-43336, Email: florian.barth@kit.edu

Abstract

In recent decades, the global cooling demand has significantly increased and is expected to grow even further in the future. However, knowledge regarding the spatial distribution of cooling demand is sparse. Most existing studies are based on statistical modelling, which lack in small-scale details and cannot accurately identify individual large cooling producers. In this study, we implement and apply a novel method to identify, map and estimate nominal cooling capacities of chillers using deep learning. Chillers typically use air-cooled condensers and cooling towers to release excess heat, and produce most of the cooling needs in the commercial and industrial sectors. In this study, these units are identified from aerial images using specifically trained object detection models. The corresponding nominal cooling capacity is then estimated based on the number of fans of air-cooled condensers and the fan diameters of the cooling towers, respectively. Both detection and capacity estimations are first evaluated on test data sets and subsequently applied to an industrial area (Brühl) and the city center in Freiburg, Germany. In Brühl, aerial images show chillers with an estimated nominal cooling capacity of 201 MW, of which the model detected 88%, while 92% of all detections are correct. In the city center, a nominal capacity of 18.6 MW is estimated, of which the model detected 87% with 77% of all detections being correct. Hence, the developed approach facilitates a reliable analysis of the installed nominal cooling capacity of individual buildings at large scales,

such as districts and cities. This information could be further used to locate areas for investments and support planning of eco-friendly, centralized supply of cooling energy, for example district heating and cooling systems or shallow geothermal energy systems such as aquifer thermal energy storage (ATES).

Keywords: Aerial images · Deep learning · Air-cooled chiller · Cooling tower · Cooling capacity · Urban energy planning

1 Introduction

According to the IEA, the demand for space cooling is "one of the most critical yet often overlooked energy issues of our time" [1]. In recent years, an increasing use of air conditioners (ACs) caused rising energy consumption as well as CO_2 emissions [2, 3, 4, 5]. Today, about 10% of global electricity consumption is related to air conditioning and mechanical ventilation [1]. In the next decades, cooling demand is expected to escalate with on-going climate change, economic growth in warmer regions and increasing living and comfort standards [1, 3, 4, 6]. Until 2050, the cooling demand of the world may triple compared to 2016 [1].

Reducing CO_2 emissions in the cooling sector requires both the use of eco-friendly technologies and the centralization of the cooling supply of urban areas [7]. Efficient technologies, such as low-temperature district heating and cooling systems and seasonal aquifer thermal energy storage (ATES) systems can significantly mitigate greenhouse gas emissions compared to conventional methods and reduce dependency on fossil fuels [8, 9, 10, 11, 12]. Other technologies for eco-friendly cooling include ground source heat pump (GSHP) systems, conventional district cooling systems, the use of waste heat, solar cooling and ice storage [13, 14, 15, 16, 17, 18, 19]. To implement such technologies on a larger scale and to design policies, information about site-specific cooling demands is needed [20, 21]. Currently the scientific

focus is mainly on modelling and quantifying heating demands, while cooling demands are often disregarded [7, 22]. However, simultaneous or seasonal heating and cooling demands in an area hold important potential for synergies and should therefore ideally be considered together [9, 11, 23].

Information about the cooling demand in Europe is rare, as energy consumption of air conditioning is not officially monitored and rather difficult to quantify [7, 20, 24, 25, 26, 27, 28, 29]. In the past, the cooling demand was modelled based on a large variety of factors. On country-scale, the installed cooling capacity and saturation rate, describing the percentage of cooled building spaces, can be estimated from the sales numbers of cooling systems [1]. However, these lack in spatial and local details. Likewise, cooling demand can be modelled top-down using factors, such as energy consumption of cities and countries, population, climate, sector distribution and national saturation rate, describing the share of buildings that use air conditioning [6, 24, 27, 29, 30, 31]. On the other hand, bottom-up approaches use small-scale factors such as building type, saturation rate, district cooling deliveries, cooling system permits, individual building energy consumption, cooling demand and floor space to extrapolate cooling demand for cities and countries [6, 21, 22, 29, 32]. However, in the EU, only a small proportion of theoretical cooling demand is met in practice with only 10% of households using air conditioning [1, 4, 20]. This low saturation rate makes it difficult to spatially quantify Europe's actually met cooling demand by using statistical models [7, 18]. While most studies focus on large areas where low AC saturation rates have less of an impact on model accuracy, the Monte Carlo models by Li et al. [22] and Chambers et al. [32] predict the present and future probability for the presence of air conditioning on building level. They use climate data and scenarios for Switzerland, data for cooling system permits, economic data, as well as floor area, service area, ground floor area and building age for individual buildings in Geneva. However, Geneva has a low saturation rate of 5-12% for cooling systems and tight regulations [22]. Thus, transferring

the approach to other regions would require adjustments to the model and other site-specific data.

By 2020, about 2 billion ACs were installed worldwide and the majority of them operate inefficiently [1, 33]. There are several configurations of ACs such as packaged ACs, split ACs and large compression chillers [1, 34]. Although, electrically driven compression chillers only make up about 2% of the ACs worldwide, they account for a large proportion of produced cooling energy due to their high cooling capacity [1, 4]. Solely in the commercial sector, about 60% of the worldwide cooling capacity is delivered by compression chillers (CCs) [1]. However, they are also frequently used to cool large residential buildings and industrial processes [1]. In Europe, 43% of the final energy consumption of the cooling sector is caused by chillers [6]. The majority of chillers are either air-cooled chillers (ACCs) or water-cooled chillers (WCCs) in combination with a cooling tower (CT) [35].

In 2021, Schüppler et al. published a workflow to identify the condenser of ACCs from aerial images and to estimate their nominal cooling capacity of the ACC from the number of build-in condenser fans [7]. Compared to other methods, this approach is based on readily available data, and the method is not limited to specific building sectors. However, manually identifying ACC condensers on city scale and counting their fans is a time-consuming task. In addition, the workflow by Schüppler et al. [7] focused on ACCs whilst disregarding WCCs.

Recently, deep learning and convolutional neural networks (CNNs) gained much attention and with major improvements in the last years they have become an important tool to find and classify objects within images, a task referred to as object detection [36, 37, 38, 39, 40]. Typically, a computer model learns how to process given data in order to make predictions for unseen data [41]. This technique is already frequently used to efficiently solve time consuming tasks such as detecting water wells, storage tanks, various vehicles, planes, boats, and certain buildings within satellite and aerial images [42, 43, 44, 45, 46, 47, 48]. In addition, previous

studies detected CTs to support the investigation of Legionnaires' disease outbreaks in the US [49].

Building on the approach of Schüppler et al. [7], this study presents a methodology to identify, map and estimate the installed cooling capacities of ACC condensers and CTs of WCCs from aerial images using deep learning. ACC condensers and the CTs are identified using state-of-the-art object detection algorithms. Using a regression analysis, the nominal cooling capacity of the identified ACC condensers and CTs is then estimated, based on the detected number of fans of ACC condensers and the fan diameter of CTs. Finally, the trained object detection models are evaluated on test data and applied to identify and map the nominal cooling capacity of ACC condensers and CTs in the industrial area of Brühl and the city center of Freiburg in Germany.

2 Methods

The workflow developed in this study comprises of four steps (Fig. 1), which are explained in the following chapters: a) data collection for training and testing by exporting aerial images from Google Earth, b) object detection of ACC condensers, ACC fans and CTs via the EfficientDet D0 algorithm [50] and the Tensorflow Object Detection API, c) quantification of cooling capacities of detected ACC condensers and CTs by means of regression analysis and d) application to a case study in Freiburg, Germany.

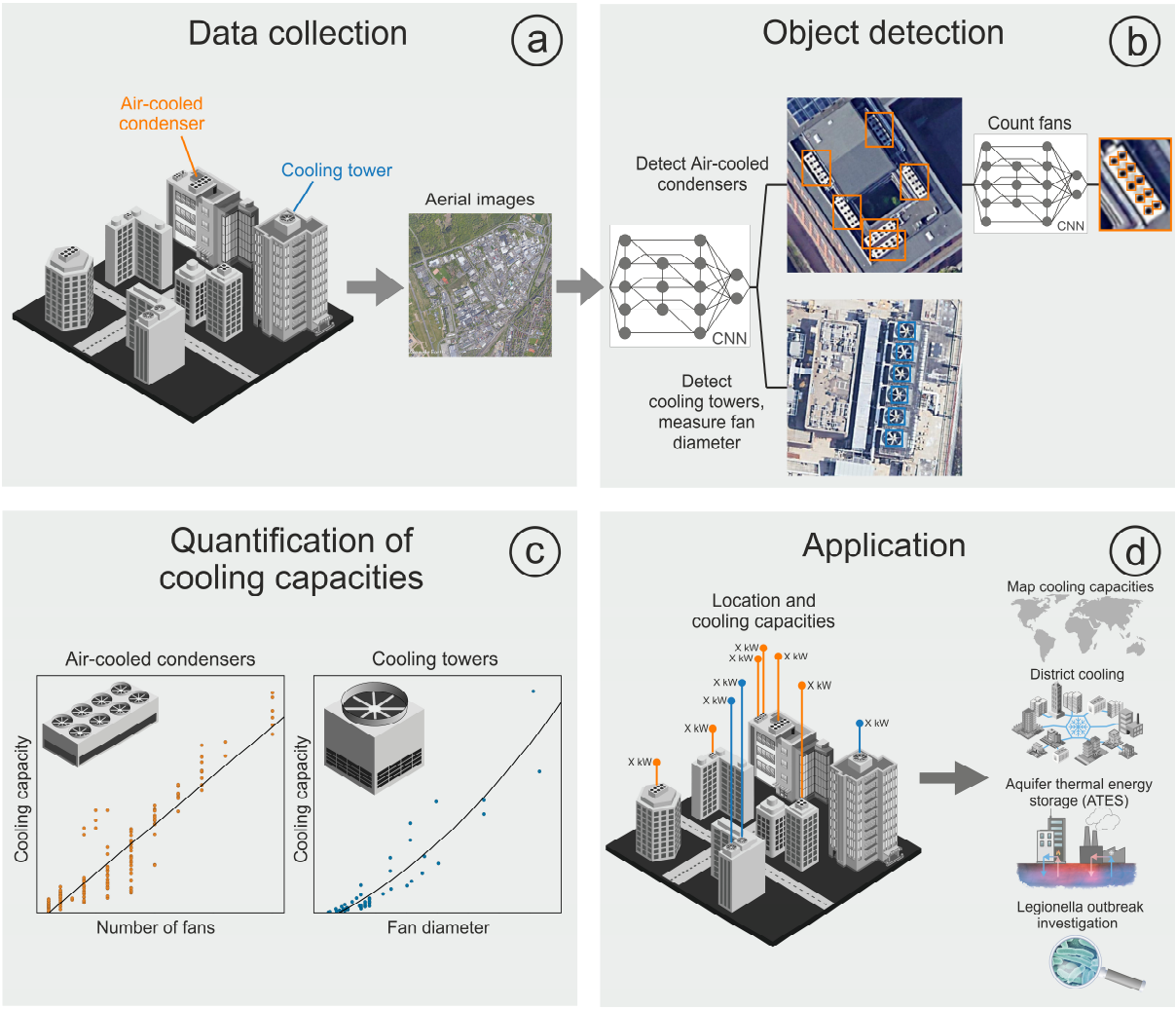

Fig. 1. Workflow for the proposed method. Aerial images are collected (a), analyzed using convolutional neural networks (b) and the nominal cooling capacity of detected air-conditioning supply is estimated (c). Thus, spatial information of cooling capacities can be gathered and used in the future to plan more efficient and eco-friendly cooling systems (d). (2 column image)

2.1 Training and test data

To train and evaluate the object detection models, a data base with images of ACC condensers, CTs and blanks is built. Hence, aerial images from various cities worldwide are used (New York City, Chicago, Tokyo, Sydney, Vienna, Rome, London, Berlin, Cologne, Frankfurt, Düsseldorf, Karlsruhe, Mannheim, Mainz, Wiesbaden, Speyer, Rüsselsheim and Rheinau). These locations are chosen due to their diversity in prevailing architecture, high number of

installed ACC condensers or CTs and availability of images with low ground sample distances of < 30 cm/pixel. The training and test images are cropped to 512 × 512 pixels (px) and ACC condensers and CTs are labelled (Fig. 1b). Each training image is rotated twice to create additional representations of each unit and 25% of the images are converted into grayscale using the tool "Roboflow" [51]. Thus, 3000 images used for training the model to detect ACC condensers and CTs.

For the CTs, only the fan is detected by the model and the bounding box corresponds to the size of the fan. To more accurately match the predicted box size with the size of the CT fans, a calibration is done using 211 CTs. To detect and count ACC condenser fans, an additional training data set is created. Images are cropped to the extent of the ACC condenser and the fans are labelled (Fig. 1b).

Similarly, a test dataset is created containing 335 ACC condensers and 145 CTs on 147 images to evaluate model performance for detecting ACC condensers and CTs, as well as estimating their cooling capacity. 46 of these images are made up of blank images with multiple, similar looking objects such as storage tanks and clarifying basins.

2.2 Object detection algorithm

To identify ACC condensers and CTs from aerial images and to count the number of fans of ACCs and measure the fan diameter of CTs, the object detection model EfficientDet D0 is used with an EfficientNet B0 backbone [50]. EfficientDet D0 was constructed by the Google Brain Team as one of eight models of the EfficientDet model family and is explained in detail by Tan et al. [50]. It is a one-stage detector that delivers high accuracy, while requiring low computational cost and therefore maintaining high detection speeds. Models are trained inside Google Colab using a Tesla T4 GPU, a batch size of 16, a learning rate of 0.001 - 0.08 and the

swish activation function [52]. The models use regularization, which prevents the model from overfitting to the exact noise pattern of an object [53].

2.3 Quantification of cooling capacities

Compression chillers are mainly used in commercial buildings, large central systems, large residential buildings and district cooling networks [1]. They absorb heat from a building space by evaporating a fluid refrigerant using a condenser unit [2]. The condenser unit can either be air-cooled or water cooled, e.g. via cooling towers to release excess heat into the environment [35]. This study is based on the principle, that larger condensers with more fans or larger cooling towers can release more heat from the chiller and therefore, the chiller can have a higher nominal cooling capacity.

2.3.1 Air-cooled condensers

Air-cooled chillers (ACCs) use ambient air to directly cool the warm refrigerant flowing through the condenser coils [35]. Thus, one or multiple fans blow air through the condenser unit (Fig. 2). Schüppler et al. [7] showed that the nominal cooling capacity of ACCs can be estimated from the number of axial fans of the external condenser unit. Hence, they created a regression analysis based on manufacturer data of 68 ACC condensers from Trane Roggenkamp and Emicon GmbH [7]. For the present study, their regression analysis is extended by 100 ACC condensers from other manufacturers such as Carrier, Galletti S.p.A., Lennox International and WITT Kältemaschinenfabrik GmbH to create a more representative database for application. The resulting relationship is used to calculate the nominal cooling capacity of ACC condensers:

$$Q_{th} = 62.1 \times N - 63.8 \quad (1)$$

with Q_{th} being the nominal cooling capacity in kW and N being the number of axial fans. Please note that only nominal cooling capacities are used within this work. For most units of the

regression, nominal capacities are certified by the manufacturers for Eurovent conditions with a fluid inlet temperature of 12°C, an outlet temperature of 7°C and an ambient air temperature of 35°C [54]. Depending on site specific operating conditions, such as refrigerant type, refrigerant and ambient air temperature and pressure and part load ratio the actual cooling capacity can differ from the nominal cooling capacity. However, to include these parameters, detailed in information about the location and the operation of each chiller would be necessary. To ensure applicability and flexibility of the approach and prevent extensive data requirements, operating parameters are not considered here.

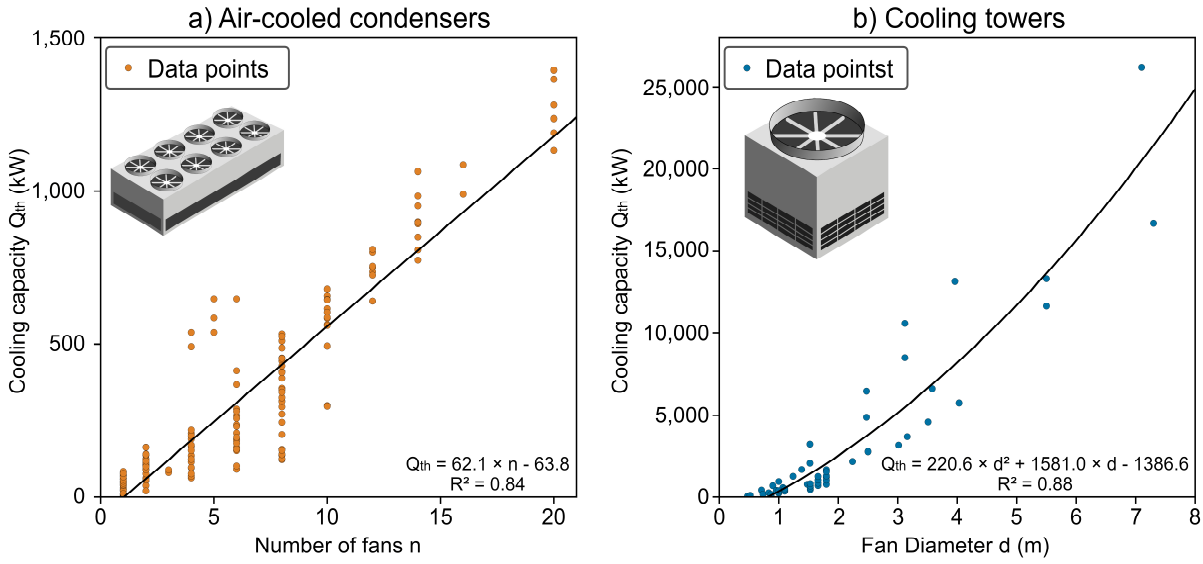

Fig. 2. Regression data for the estimation of the nominal cooling capacity of air-cooled condensers and cooling towers. The nominal cooling capacity of air-cooled condensers is correlated with the number of built-in fans and the nominal cooling capacity of cooling towers with their fan diameter. (2 column image)

2.3.2 Water-cooled chillers

Water-cooled chillers (WCCs) use cold water instead of ambient air to cool the refrigerant in the condenser unit. Typically, a CT outside of the building is used to supply cold water to the

condenser unit of the WCC [35]. WCCs and their CTs can reject more heat (Fig. 2) and are more energy efficient than ACCs [34, 55]. In this study we are focussing on the wet induced draft CT which is the most frequently used type of CT [55]. Warm water coming from the CC's condenser is sprayed onto the porous CT fill through which the water flows downwards [56]. A large fan on top of the CT induces a counterflow of air through the fill [57]. The water is then cooled on contact with the air due to evaporation and thermal conduction [56]. In general, the larger the CT, the more heat it can reject (Fig. 2). For this study, the diameter of the CT fan is used to estimate the nominal cooling capacity of the CT and therefore the chiller. The fan is also the most prominent and an easy to identify visual feature of the CT from aerial images. Using data from 53 CT models by manufacturers Cooling Tower Systems Inc., EWK, GEA Group AG, Mumme-Cooling Tower International GmbH and SPX Cooling Technologies Inc., a regression analysis is performed to estimate the nominal cooling capacity based on the fan diameter (Fig. 2). The resulting relationship is used to calculate the nominal cooling capacity within this study:

$$Q_{th} = 220.6 \times d^2 + 1518.0 \times d - 1386.6 \quad (2)$$

With d being the fan diameter in m. For most CTs, nominal cooling capacities are stated by the manufacturers for an inlet water temperature of 35°C, an outlet temperature of 30°C and wet bulb temperatures between 21°C and 25°C. Comparable to ACCs, the actual cooling capacity of CTs and the connected WCCs depends on the operating conditions, such as CT fan speed, inlet, outlet and wet bulb temperatures and refrigerant and air pressure, which are again not considered in the approach for sake of applicability and flexibility.

2.3.3 Evaluation metrics and calibration

After training, the object detection model is evaluated on the test data set using different evaluation metrics. A summary over the used evaluation and calibration metrics for the individual steps and algorithms of the workflow is given in Table 1.

Tab. 1. Evaluation metrics for the object detection models for the different workflow tasks (Fig. 1 b & c). For the evaluation of the object detection (B), an intersection over union (IoU) > 0.5 is used as criteria to distinguish true positive detections from false negatives and the mean average precision (mAP) is calculated from the precision-recall-curve. Manual judgement omits the use of IoU, whereas detections are rated intuitively as true and false. For the estimation of nominal cooling capacities (C), eq. 1. and eq. 2. are used to calculate the model's estimated and actual nominal cooling capacity.

Task			Criteria	Evaluation Metrics
b)	Object detection		Location of ACCs and CTs	IoU: precision-recall-curve, mAP
				Manually judged: F1-score, number of included ACC fans
c)	Quantification of cooling capacities		Cooling capacity from number of fans	Total capacities, mean relative deviation
b) + c)	Quantification of cooling capacities	ACC Evaluation	Cooling capacity from number of fans	Total capacities, prediction interval
		CT Calibration	Cooling capacity from fan size	Mean relative deviation
		CT Evaluation	Cooling capacity from fan size	Total capacities, prediction interval

For the detection of ACC condensers and CTs, the mean average precision (mAP) is calculated following the Pascal VOC 2012 metrics by Everingham and Winn [58] using a Python implementation by Cartucho et al. [59]. The mAP is a common evaluation metric in object detection and is calculated from the precision-recall curve. The precision provides a measure

for how accurate the given detections are, while the recall describes how many existing objects are correctly detected [60]. To calculate precision and recall, the following equations are used:

$$Precision = \frac{TP}{TP + FP} \tag{3}$$

$$Recall = \frac{TP}{TP + FN} \tag{4}$$

with *TP* being the number of true positive detections, *FP* being false positive detections and *FN* being false negative detections [60]. For Pascal VOC 2012, TPs are judged using an intersection over union (IoU) > 0.5 [59]. However, our model might have difficulties to correctly distinct between multiple, clustered ACCs. Yet, precisely separating each ACC condenser in a cluster of multiple units is rather subsidiary compared to including the correct number of fans. Hence, we additionally evaluate performance manually by judging TPs, FPs and FNs intuitively, instead of using IoU (Tab. 1). If the model includes multiple ACC condensers inside a single bounding box, all are considered as TPs, as long as the majority of fans are included. To compare performance, the F1-score is calculated from the number of included ACC fans after Sammut and Webb [61] as follows:

$$F1 = \frac{2 \times (Precision \times Recall)}{Precision + Recall} \tag{5}$$

To verify the regression analysis for the estimation of the cooling capacity of ACCs, we calculate the nominal cooling capacity of ACCs in the study area used by Schüppler et al. [7] using eq. 1. and compare them to the actual installed nominal capacities. The study area is located at the Campus North of the Karlsruhe Institute of Technology (KIT).

The nominal cooling capacity of ACCs is calculated from the detected number of condenser fans by the second model. Evaluation for this step is done using all detected ACCs from the test data set with TPs and FPs. The cooling capacities calculated from the number of true fans and the models estimated number of fans are compared.

Regarding the CTs, the nominal cooling capacity estimation is additionally calibrated before model evaluation. Hence, the models estimated fan diameters of CTs in the calibration set are compared to the true diameters. The model's capability to estimate the nominal cooling capacity of CTs is rated in terms of how precise the model can predict the size of the CT fans in the test data set after calibration. From true and estimated diameters, the nominal cooling capacity is calculated using eq. 2.

2.4 Application in the city of Freiburg

In addition to evaluating the individual model stages using dedicated test data, the combined detection and regression models are applied to two study areas in the city of Freiburg, Germany, namely the industrial area of Brühl (3.8 km^2) and the city center (2.4 km^2) (Fig. 3). The areas are chosen due to their diversity of installed unit types and sizes, building types, architecture and availability of high-resolution aerial images. For both areas, aerial images are exported from Google Earth with a GSD of 10 cm and tiled down into thousands of smaller images. To filter out objects that are detected multiple times in the overlap areas, a non-max suppression algorithm is used. For this study, we focus on ACCs with two or more fans while ignoring small units with one fan.

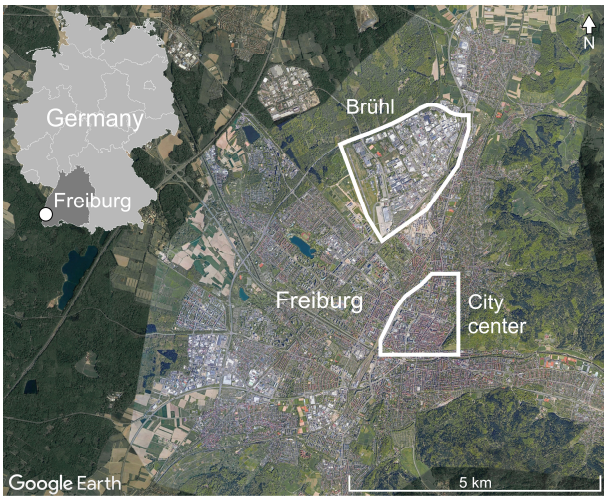

Fig. 3. Study areas for the evaluation of the trained models in the industrial area of Brühl and the city center of Freiburg, Germany. (1 column image)

3 Results and discussion

3.1 Detection of air-cooled condensers and cooling towers

The model for the detection of ACC condensers and CTs reaches peak performance after about 400 epochs of training. Performance is heavily influenced by image quality and the respective unit type (Fig. 4). Larger ACC condensers are detected more frequently and with higher confidence than smaller ones. Large ACC condensers have multiple fans arranged in an easily recognisable fan pattern (Fig. 1a), while small ACC condensers often show few features for the model to characterize them properly (Fig. 1b), especially when using regularization. If fan blades of CTs are not visible, e.g. due to unit type, motion blur, atmospheric distortion, dark painted blades or a high number of blades per fan, the CT is more likely to remain undetected (Fig. 4d).

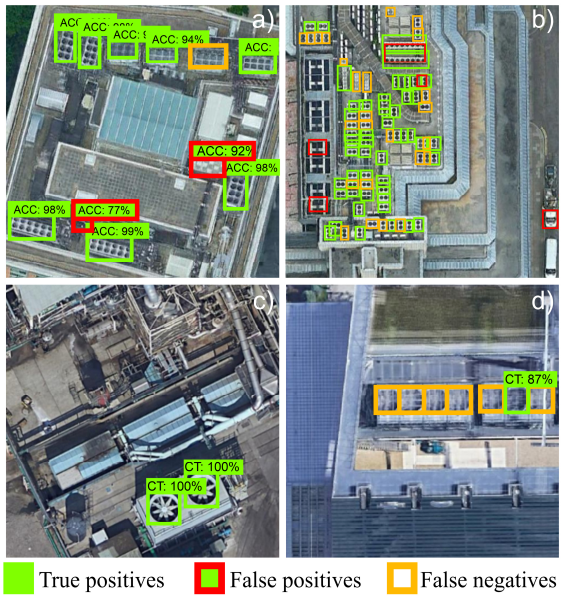

Fig. 4. Examples for the detection of condensers of air-cooled chillers (ACCs) (a, b) and cooling towers (CTs) (c, d). True positives are correctly detected condensers or CTs, false positives are other objects falsely classified as condensers or CTs and false negatives are undetected condensers or CTs. (1 column image)

Overall, the detection of CTs produces better results than the detection of ACCs. ACC condensers are detected with an AP of 78.6%, CTs with an AP of 93.4%, resulting in a mAP of 86.0% (Fig. 5). Direct comparison of our model with other studies focussing on object detection within aerial images is difficult due to differing object classes, availability of training data and GSD. In general, our model's mAP is similar to models trained on aerial images from other research. The Multi-Scale CNN by Guo et al. [43] achieves a mAP of 89.6%, the Faster R-CNN and SSD models by Mansour et al. [45] achieve 89.2% and 84.2% and the YOLO based model by Haroon et al. [44] achieves 60.9%. However, most objects detected in these studies are significantly larger and therefore easier to detect for a CNN than many small ACC condensers in our study [43, 44, 45].

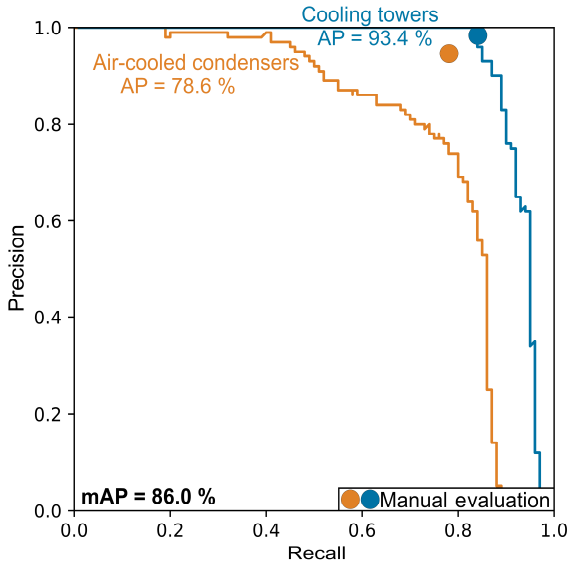

Fig. 5. Precision-recall curve of the detection of the condensers of air-cooled chiller (ACCs) and cooling towers (CTs) of water-cooled chillers, generated after the Pascal VOC 2012 metrics [58]. In addition, precision-recall values from a manual evaluation are plotted at confidence thresholds of 0.3 (ACCs) and 0.5 (CTs). (1 column image)

Manual evaluation reveals the downside of judging TPs by IoU. The best performance trade-off can be observed at a confidence threshold of 0.3 for ACCs and 0.5 for CTs. While there is no difference for CTs, manual evaluation leads to significantly better results for ACC condensers (Fig. 5), with an increased precision from 0.80 to 0.95 and recall from 0.72 to 0.79. The detection of ACC condensers shows an F1-score of 0.85 and the detection of CTs and F1 of 0.91. If judged by the number of included ACC-fans instead of the entire ACC condensers, the recall value increases further to 0.90, because larger ACC condensers with more fans are detected more frequently than smaller ones. This results in an F1 of 0.94 for ACC condensers judged by included fans.

Our EfficientDet D0 model achieves similar performance at detecting CTs as Towerscout's YOLOv5 model, which achieves a precision of 0.90, a recall of 0.95 and an F1 of 0.93 [49]. While the developers of Towerscout deemed recall to be more important than precision to

assure that every possible legionnaires' disease source is included, for our application we consider a high precision as critical [49]. Sacrificing precision for recall would create a large number of FPs during application that may overshadow TPs in most application areas.

3.2 Estimating cooling capacities

3.2.1 Air-cooled chillers

The regression analysis for ACCs is first used to calculate the nominal cooling capacity of ACCs for the study site at the university campus of the KIT [7]. On the campus, 36 ACCs by manufacturers Emicon and Trane are used for evaluation with a total nominal cooling capacity of 16.5 MW [7]. All units have visible condensers on the outside of the respective buildings. While the previous study overestimated the total capacity by 17% with mean relative deviation of 36% per chiller, our extended regression improves the performance with a total overestimation of 13% and an average deviation of 26% by using data from additional manufacturers.

Using our collected aerial image data set from multiple cities, the EfficientDet model for the detection of ACC fans is trained for about 50 epochs. With a confidence threshold of 0.3, the model correctly estimates the number of fans for 64% of the ACC condensers (Fig. 6). For the remaining 36% the model over- or underestimated the number of fans. Converted to cooling capacity using eq. 1, 95% of the estimations are within a prediction interval of ± 218 kW. Overall, the total nominal cooling capacity of ACC condensers in the data set is overestimated by 3%. As with the detection of ACC condensers and CTs, fan detection performance is heavily influenced by image quality and background. Most ACC condenser fans appear as dark spots, giving few optical features for the model to learn. Thus, shadows or other dark objects next to the ACCs can confuse the detection and lead to FPs.

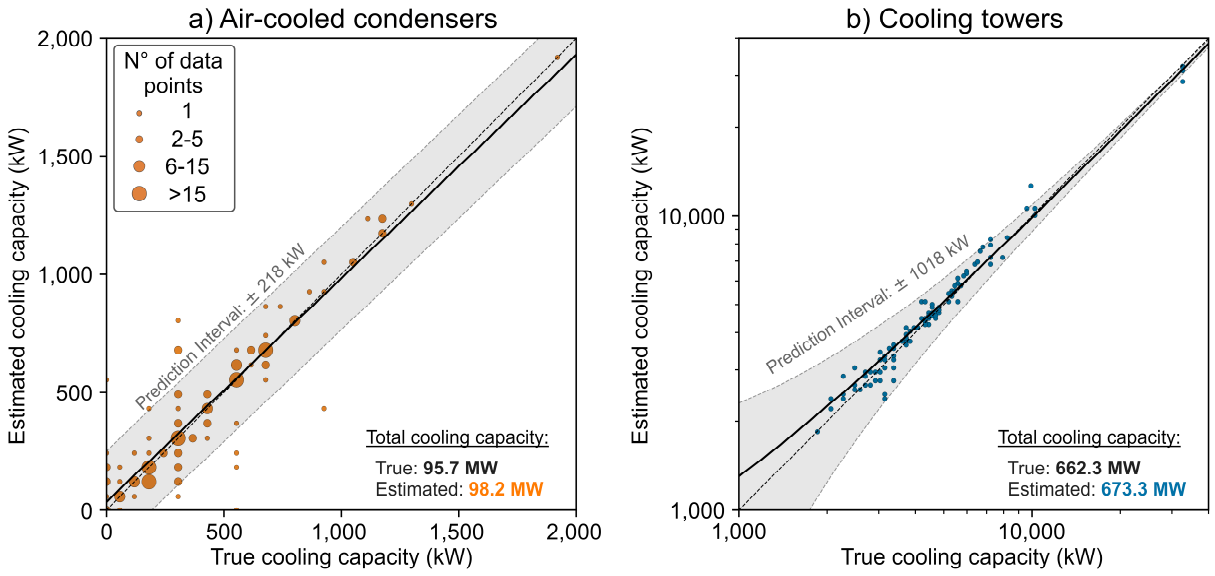

Fig. 6. Estimated and true nominal cooling capacities of the air-cooled condensers and cooling towers in the test data set. True cooling capacities are calculated from the true number of fans using eq. 1. (2 column image)

3.2.2 Cooling towers

The nominal cooling capacity of CTs is calculated from the size of the detected bounding box. Before calibration, the model overestimates the size of all CT fans in the calibration set by a mean of 16%. Both the line of best fit and a factor of 0.86, calculated from the average overestimation, are used to correct the estimations. Evaluation on the test data set shows that using the calibration factor achieves better results than the calibration function. Using the factor, the total cooling capacity of CTs in the data set is overestimated by 2% (Fig. 6). Converted to nominal cooling capacity using eq. 2, 95% of the estimations are within a prediction interval of ± 1018 kW.

3.3 Application on study areas in Freiburg

Beside applying evaluation metrics, the performance of the approach is tested and applied on two study sites in the city of Freiburg (Fig. 3). The initial application resulted in a relatively high number of FPs and a low precision compared with the test data, due to a busy background with a large number of similar looking objects within thousands of images compared to a small number of true objects. To avoid FPs while still detecting the majority of units, the confidence thresholds are increased to 0.8 for ACC condensers and 0.6 for CTs.

3.3.1 Industrial area of Brühl

In the industrial area of Brühl, 117 ACC condensers and 27 CTs are visible from aerial images. In Brühl the majority of detections is correct and the model's estimated nominal cooling capacities match the observations very well (Fig. 7). Overall, 70% of the visible units are detected with a precision of 84% (Tab. 2). However, from a total estimated nominal cooling capacity of 201.5 MW in the area, 88% are detected with a precision of 88% (Tab. 2). This includes undetected and false positive ACC condensers and CTs, incorrect numbers of ACC condenser fans and over- or underestimated CT-fan sizes. The detection of CTs works better than detection of ACC condensers with both a higher precision and recall (Tab. 2). With an F-score of 0.89 our model shows similar performance at detecting CTs as Towerscout tested in Seattle (F1 = 0.90) and Athens (F1 = 0.86) [49]. Overall, considering that no training images from Freiburg are used, the model was well capable to generalize the optical features of ACC condensers and CTs during training and subsequently recognize them in Freiburg.

Tab. 2. Total number and nominal cooling capacities (Q_{th}) of observable condensers of air-cooled chillers (ACCs) and cooling towers (CTs) in the application areas in Freiburg. Total observable nominal capacities are compared to true positive (TP), False positive (FP) and False Negative (FN) capacities detected by the models.

Study area	Unit type	Observable		True positive		False positive		False negative	
		N° of units	Q_{th} (kW)	N° of units	Q_{th} (kW)	N° of units	Q_{th} (kW)	N° of units	Q_{th} (kW)
Brühl	ACC condensers	117	27.5	78	19.3	18	5.6	39	8.3
	CTs	28	174.0	24	162.0	2	19.6	4	15.4
	Total	**145**	**201.4**	**102**	**181.2**	**20**	**25.1**	**43**	**23.6**
City center	ACC condensers	79	18.6	57	16.2	15	4.8	22	2.4
	CTs	0	0	0	0	20	74.2	0	0
	Total	**79**	**18.6**	**57**	**16.2**	**35**	**78.9**	**22**	**2.4**
	Total (if evaporative chillers are CTs)	85	26.5	57	16.2	35	78.9	28	10.3

Most FNs are undetected machines that are either difficult to spot due to shadows or low contrast, or are comparatively small. Particularly small ACC condensers with only two fans often remain undetected. Yet, at the same time, their nominal cooling capacity is relatively small so that the resulting error in the overall estimated nominal cooling capacity is also small. The largest portion of undetected nominal cooling capacity is due to undetected CTs (Fig. 7 A). They are partly covered by steam, which makes them difficult to identify even for the human eye. Overestimated CT-sizes account for the largest portion of false positive nominal cooling capacity (Fig. 7 A) followed by false positive CTs in the form of two misclassified storage tanks (Fig. 7 B). Another 17 objects, such as skylights, construction materials and vehicles are falsely classified as ACC condenser, accounting for a false positive nominal cooling capacity of 5.6 MW.

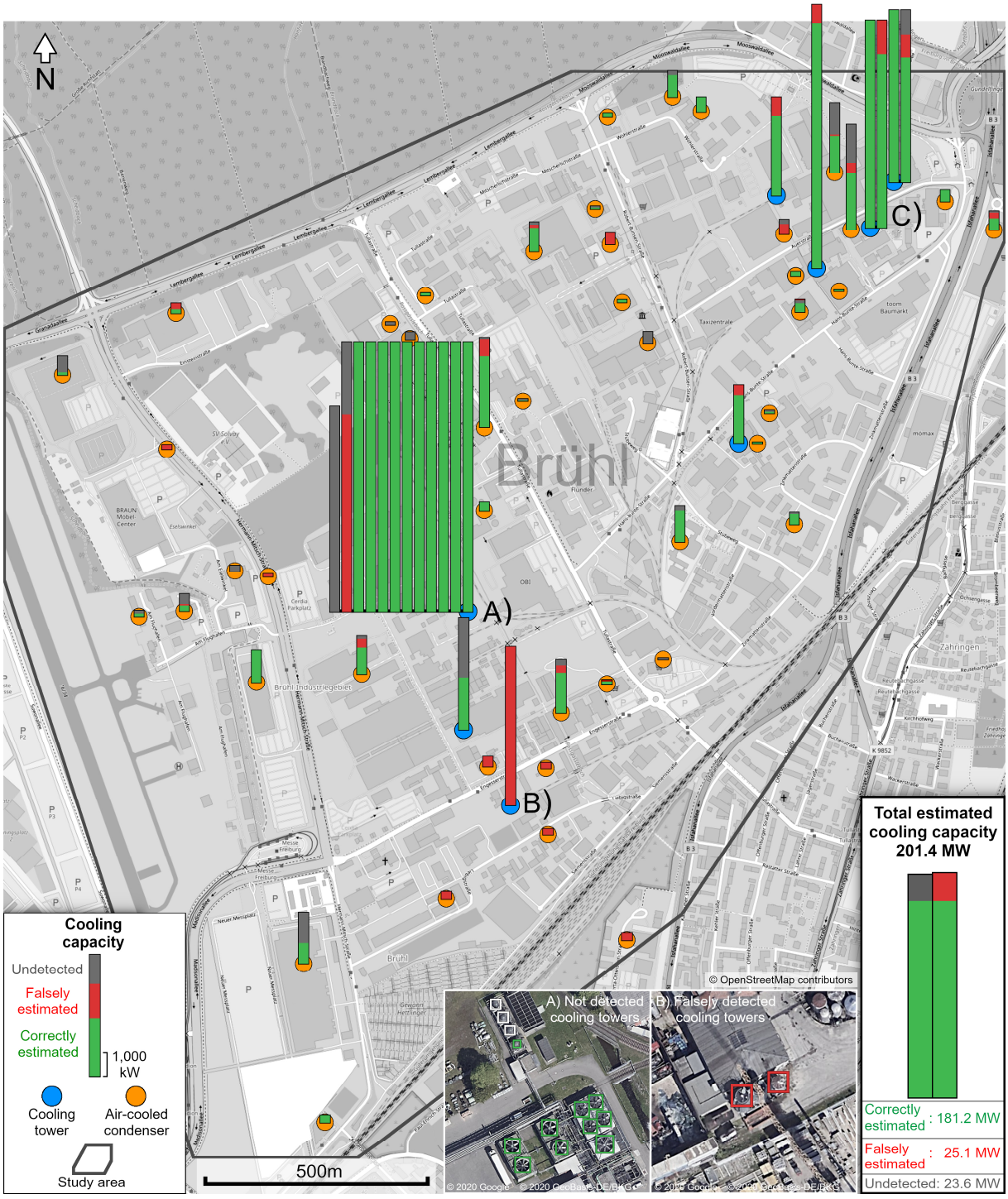

Fig. 7. Results for the estimation of nominal cooling capacities in the industrial area of Brühl in the city of Freiburg, Germany. Bars represent the nominal cooling capacity at each location. Multiple units on the same building are summed up. Some detections are highlighted for discussion (A-C). (2 column image)

Overall, the aerial image analysis in Brühl identified two areas with particularly high nominal cooling capacities which include a large an industrial park (Fig. 7 A) and two factory sites (Fig. 7 C). In the industrial park, multiple large CTs are installed, while in the two factory sites a combination of ACC condensers and smaller CTs are identified. Thus, these two areas would be areas of interest for further investigations regarding eco-friendly production of cooling energy. Furthermore, feasibility for waste heat utilisation and storage for nearby quarters and buildings should be verified.

3.3.2 City center

In the city center 79 ACC condensers are visible from aerial images. The model performance for detecting both ACC condensers and CTs in the city center drops significantly compared to the industrial area. With a total nominal cooling capacity of 18.6 MW, the model correctly detected 87% (Tab. 2). However, the model misclassified 20 objects as CT and estimated a false nominal cooling capacity of 74.2 MW resulting in a low precision of 17%. In reality, most alleged CTs are skylights or concrete and grass patterns on the ground (Fig. 8 B, C). If only ACC condensers were detected and the detection of CTs was intermitted, precision could be increased to 77%. During data acquisition, we rarely observe the use of CTs other than for industrial processes in Germany. Hence, besides retraining the model, omitting the detection of CTs in areas without industrial buildings and solely focussing on ACC condensers might be a valid strategy to avoid FPs in dense urban areas. For ACC condensers, the majority of FP nominal cooling capacity is caused by intersecting bounding boxes, which results to fans being counted twice (Fig. 8 A).

In addition to the previously discussed chillers, three units with an ambiguous type of cooling are visible on top of three university buildings (Fig. 8 D, E and F). Optical similarities suggest either hybrid evaporative chillers or cooling towers. Both possibilities are considered. In case the chillers are CTs, the potential nominal cooling capacity would be estimated as 7.9 MW.

Because our model does not detect them as CTs, the FN nominal cooling capacity in the area would increase significantly.

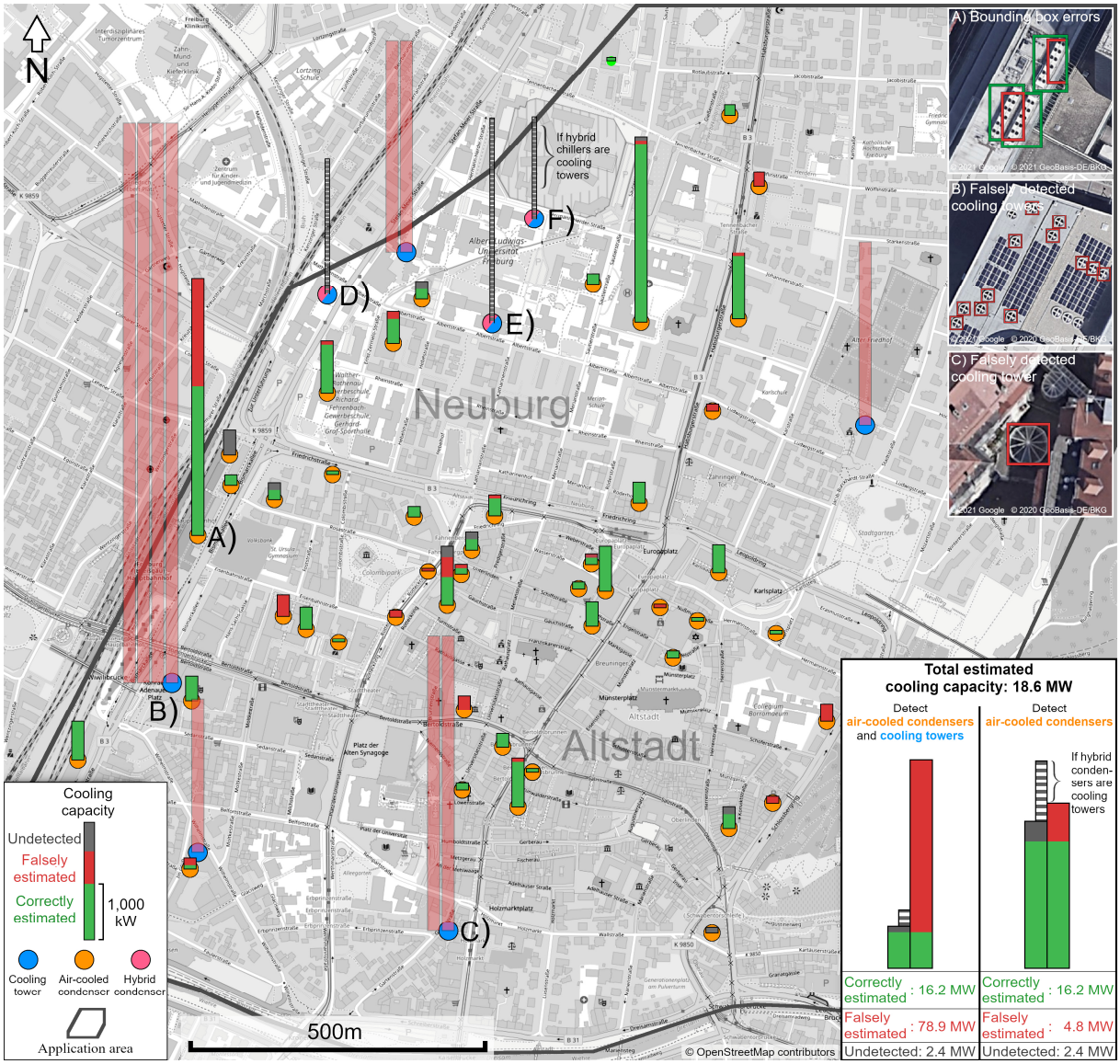

Fig. 8. Results for the estimation of nominal cooling capacities in the city center of Freiburg, Germany. Bars represent the nominal cooling capacity at each location. Multiple detections that belong to the same building are summed up. Locations A-C are highlighted for discussion. For the locations D), E) and F), the possibility that installed chillers are cooling towers instead of hybrid chillers is considered, as well. (2 column image)

While overall capacities are lower than in Brühl, there are some areas of interest in the city center for possible investigation for an eco-friendly production of cold. These include

healthcare facilities and several research and educational institutions (Fig. 8 D, E and F), as well as the main station (Fig. 8 A) and several smaller buildings where cooling energy is currently produced by electric chillers. A groundwater cooling circuit, as already installed on the university campus nearby, might be a valid option to reduce energy consumption of air conditioning in these areas [62]. Otherwise, as most of these buildings likely require both heating in winter and cooling in summer, seasonal aquifer thermal energy storage (ATES) might be a feasible option, as well [8].

3.4 Comparison and limitations

Comparing results from our approach with previous studies proves to be difficult as most of these focus on estimating theoretical cooling demand (e.g. [6, 22, 24, 27, 28, 29, 31, 32]). While the cooling demand could be estimated from the nominal cooling capacity by assuming different operational parameters, such as operating hours and part load ratios, and adjusting for local climatic conditions, this is beyond the scope of this study.

In contrast to most of these studies (e.g. [22, 24, 27, 28, 29]), our approach is not limited to a specific sector. Hence, the method is a suitable addition to other approaches, such as building stock models, e.g. to include industrial cooling demand. Likewise, our approach achieves a much higher spatial resolution (i.e. on building level). While some statistical models may be projected at a grid size down to 100 m, the confidence for areas below 1 km is low [29, 63]. Other models predict the presence of air-conditioning based on building properties specific for Switzerland [22; 32]. On the other hand, our current approach is widely applicable and could therefore help to verify the presence of air-conditioning equipment in order to increase accuracy and to adjust the former models to different countries.

While our method is able to detect the two most frequently used heat rejection units of chillers, air-cooled condensers and induced draft CTs, the current models are not yet able to detect,

distinguish and process other units, such as forced draft CTs, adiabatic condensers, condensers of absorption chillers or packages systems, such as rooftop units. As these units are more difficult to spot and differentiate on aerial images, new object detection models have to be trained and additional regression analyses are needed in order to incorporate them.

The currently low performance of detecting small ACC condensers with one fan might be improved by extending the training data set with additional images of small units, increasing image resolution or using a different model architecture. Intersecting and unprecise bounding boxes can be avoided. In instance segmentation, each pixel of an image is classified, making it possible to more accurately detect the extent of contained object [64]. However, if units are covered by roofs or vegetation, or if they use radial fans instead of axial fans, they cannot be currently detected.

As shown in Fig. 2, different chillers may deliver different cooling capacities while having an equal number of fans or fan diameter. Accordingly, these optical parameters only provide an initial estimate of the nominal cooling capacity. Likewise, it is impossible to assess, whether a unit is used for free cooling or in compression mode. As mentioned above, operational parameters, such as fan speeds, internal pressures, temperatures and type of refrigerant also have an impact on the cooling capacity. Thus, our current estimated nominal cooling capacity will differ from the actual cooling capacity and the required cooling load.

4 Conclusion

In this study, we presented a method to identify and map air-conditioning equipment on rooftops from aerial images and quantify their nominal cooling capacity based on their optics and dimensions. We trained object detection models to identify the condensers of air-cooled chillers and their fans, as well as the fan of cooling towers. Based on the number of fans of air-cooled condensers and the fan diameter of cooling towers the nominal cooling capacity is estimated.

We successfully evaluated our method on a set of test images and known nominal cooling capacities of chillers and apply them to two districts in the city of Freiburg in Germany. Chillers in the test data set are detected with a mean average precision (mAP) of 86%. The number of condenser fans and cooling tower fan size, which correspond to their nominal cooling capacity, is overestimated by only 2%. When comparing our estimations with known installed nominal cooling capacities of chillers in a study area, the total nominal cooling capacity is overestimated by 13%. During the application to the city of Freiburg, the models were able to correctly detect 88% of installed nominal cooling capacity (recall value) in the industrial area of Brühl, while 88% of the model's assertions were correct (precision value). In the future, the method can be further enhanced by integrating additional types of heat rejection units and air-conditioners allow for a more comprehensive evaluation of installed nominal cooling capacities in all building sectors. To further increase applicability, a correction should be introduced depending on prevailing climate conditions. Furthermore, the regression analysis should be validated for each additional chiller type using installed chillers in addition to manufacturer data sheets.

Our detection method can support the transition from conventional heating and cooling systems to more innovative and sustainable systems. It can provide valuable information about the cooling sector at each scale without extensive data requirements, for example for developing cooling cadastres of potential heat sources and sinks. This information can then be used to locate possible recipients of eco-friendly cooling technologies, or not utilized waste heat sources for the planning of district heating and cooling systems and aquifer thermal energy storage systems [8, 9].

Data availability

Data, code and trained object detection models will be made available upon acceptance.

Acknowledgements

The financial support for Kathrin Menberg via the Margarete von Wrangell program of the Ministry of Science, Research and the Arts (MWK) of the State of Baden-Württemberg is gratefully acknowledged. Thanks also go to Stefan Hinz (Karlsruhe Institute of Technology, Institute of Photogrammetry and Remote Sensing), Sven Eckhardt (Amazon Science) and Nico Peter (Karlsruhe Institute of Technology, Department of Informatics) for their expertise on remote sensing and deep learning.

References

[1] IEA, 2018. The Future of Cooling: Opportunities for energy-efficient air conditioning, IEA, Paris. https://doi.org/10.1787/9789264301993-en.

[2] Blesl, M. and Kessler, A., 2017. Energieeffizienz in der Industrie. 2. Auflage. Springer Vieweg, 2017. ISBN 978-3-662-55998-7.

[3] García Cutillas, C., Ruiz Ramírez, J. and Lucas Miralles, M., 2017. Optimum Design and Operation of an HVAC Cooling Tower for Energy and Water Conservation. Energies. 10, 299. https://doi.org/10.3390/en10030299.

[4] IEA, 2021. Cooling, IEA, Paris https://www.iea.org/reports/cooling (accessed 01.12.2021).

[5] Pereira, G. da S., Primo, A. R. and Villa, A. A. O., 2015. Comparative study of air conditioning systems with vapor compression chillers using the concept of green buildings. Acta Scientiarum. Technology. 37(4), 339–346. https://doi.org/10.4025/actascitechnol.v37i4.27390.

[6] Kranzl, L., Hartner, M., Müller, A., Resch, G., Fritz, S., Fleiter, T., Herbst, A., Rehfeldt, M., Manz, P., Zubaryeva, A. and Gomez Vilchez, J., 2018. Hotmaps. Heating and Cooling outlook until 2050, EU-28. Update March 2019.

[7] Schüppler, S., Fleuchaus, P., Zorn, R., Salomon, R. and Blum, P., 2021. Quantifying Installed Cooling Capacities Using Aerial Images. PFG - Journal of Photogrammetry, Remote Sensing and Geoinformation Science. 89, pages 49–56. https://doi.org/10.1007/s41064-021-00137-0.

[8] Fleuchaus, P., Godschalk, B., Stober, I. and Blum, P., 2018. Worldwide application of aquifer thermal energy storage - A review. Renewable and Sustainable Energy Reviews. 94, 861-876. https://doi.org/10.1016/j.rser.2018.06.057.

[9] Lund, H., Østergaard, R.A., Nielsen, T.B., Werner, S., Thorsen, J.E. Gudmundsson, O., Arabkoohsar, A. and Vad Mathiesen, B., 2021. Perspectives on fourth and fifth generation district heating. Energy, 227. https://doi.org/10.1016/j.energy.2021.120520.

[10] Patyn, J. and Lookman, R., 2012. The combination of aquifer thermal energy storage (ATES) and groundwater remediation. CityChlor Cooperation. https://www.citychlor.eu/sites/default/files/citychlor_ates_with_remediation_20april2012.pdf (accessed 17.03.2022.).

[11] Schüppler, S., Fleuchaus, P. and Blum, P., 2019. Techno-economic and environmental analysis of an Aquifer Thermal Energy Storage (ATES) in Germany. Geothermal Energy. 7. https://doi.org/10.1186/s40517-019-0127-6

[12] Stemmle, R., Blum, P., Schüppler, S., Fleuchaus, P., Limoges, M., Bayer, P. and Menberg, K., 2021. Environmental impacts of aquifer thermal energy storage (ATES). Renewable and Sustainable Energy Reviews. 151, 111560, ISSN 1364-0321, https://doi.org/10.1016/j.rser.2021.111560.

[13] Chan, A.L.S., Chow, T.-T., Fong, S.K.F. and Lin, J.Z., 2006. Performance evaluation of district cooling plant with ice storage. Energy. 31(4), 2750–2762. ISSN 0360-5442, https://doi.org/10.1016/j.energy.2005.11.022.

[14] Eveloy, V. and Ayou, D. S., 2019. Sustainable District Cooling Systems: Status, Challenges, and Future Opportunities, with Emphasis on Cooling-Dominated Regions. Energies. 12(2), 235. https://doi.org/10.3390/en12020235.

[15] Gruber-Glatzl, W., Krainz, R., Fluch, J., Mauthner, F., Hammer, A., Lachner, E., Kienberger, T., Hummel, M. and Müller, M., 2020. Abwärmekataster III Steiermark. Öffentlicher Kurzbericht. Version 2.0. https://www.aee-intec.at/0uploads/dateien1573.pdf (accessed 18.05.2022).

[16] Santin, M., Chinese, D., De Angelis, A. and Biberacher, M., 2020. Feasibility limits of using low-grade industrial waste heat in symbiotic district heating and cooling networks. Clean Technologies and Environmental Policy. 22, 1339–1357. https://doi.org/10.1007/s10098-020-01875-2.

[17] Stauffer, F., Bayer, P., Blum, P., Giraldo Molina, N. and Kinzelbach, W., 2013. Thermal use of shallow groundwater, 1st. ed. CRC Press, Boca Raton. https://doi.org/10.1201/b16239.

[18] Tiwari, G.N., Tiwari, A. and Shyam, 2016. Solar Cooling, in: Handbook of Solar Energy. Energy Systems in Electrical Engineering. Springer, Singapore. pp 471–487. https://doi.org/10.1007/978-981-10-0807-8_11.

[19] Yan, C., Shi, W., Li, X. and Zhao, Y., 2016. Optimal design and application of a compound cold storage system combining seasonal ice storage and chilled water storage. Applied Energy. 171, 1–11. ISSN 0306-2619. https://doi.org/10.1016/j.apenergy.2016.03.005.

[20] Möller, B., 2015. Mapping the Heating and Cooling Demand in Europe. Work Package 2. Background Report 5.

[21] Werner, S., 2016. European space cooling demands. Energy. 110 (C), 148–156. DOI: 10.1016/j.energy.2015.11.028.

[22] Li, X., Chambers, J., Yilmaz, S. and Patel, M.K., 2021. A Monte Carlo building stock model of space cooling demand in the Swiss service sector under climate change, Energy and Buildings. 233, 2021, 110662, ISSN 0378-7788, https://doi.org/10.1016/j.enbuild.2020.110662.

[23] De Oliveira, F., Schneider, S. and Hollmuller, P., 2019. DataRen, a Territorial Energy Demand Modelling Tool. IOP Conference Series: Earth and Environmental Science. 290 012093. DOI: 10.1088/1755-1315/290/1/012093.

[24] Asloune, H., Riviere, P., Dittmann, F. and Berthou, T., 2019. Modelling, Prospective Modelling of Residential Space Cooling Diffusion in France. https://hal-mines-paristech.archives-ouvertes.fr/hal-02066476.

[25] Fleiter, T., Steinbach, J., Ragwitz, M., Arens, M., Aydemir, A., Elsland, R., Frassine, C., Herbst, A., Hirzel, S., Krail, M., Rehfeld, M., Reuter, M., Dengler, J., Köhler, B., Dinkel, A., Bonato, P., Azam, N., Kalz, D., Toro, F. A., Gollmer, C., …Naefeli, C., 2016a. Mapping and analyses for the current and future (2020 - 2030) heating/cooling fuel development (fossil/renewables). Executive summary. Fraunhofer ISI, Frauhofer ISE, TU Wien, TEP Energy, IREES, Observer.

[26] Fleiter, T., Steinbach, J., Ragwitz, M., Arens, M., Aydemir, A., Elsland, R., Frassine, C., Herbst, A., Hirzel, S., Krail, M., Rehfeld, M., Reuter, M., Dengler, J., Köhler, B., Dinkel, A., Bonato, P., Azam, N., Kalz, D., Toro, F. A., Gollmer, C., …Naefeli, C., 2016b. Work package 1: Final energy consumption for the year 2012. Fraunhofer ISI, Frauhofer ISE, TU Wien, TEP Energy, IREES, Observer.

[27] Jakubcionis, M. and Carlsson, J., 2017. Estimation of European Union residential sector space cooling potential. Energy Policy. 101, 225–235. ISSN 0301-4215. https://doi.org/10.1016/j.enpol.2016.11.047

[28] Jakubcionis, M. and Carlsson, J., 2018. Estimation of European Union service sector space cooling potential. Energy Policy. 113, 223–231. https://doi.org/10.1016/j.enpol.2017.11.012.

[29] Persson, U. and Werner, S., 2015. Quantifying the Heating and Cooling Demand in Europe. Work Package 2. Background Report 4.

[30] Frayssinet, L., Merlier, L., Kuznik, F., Hubert, J.-L., Milliez, M., Roux, J.-J., 2018. Modeling the heating and cooling energy demand of urban buildings at city scale. Renewable and Sustainable Energy Reviews. 81(2), 2318–2327. 10.1016/j.rser.2017.06.040. hal-01842364.

[31] Unternehmen für Ressourcenschutz, 2010. Kältemarktanalyse der Stadt Hamburg im Juni 2010. 20355 Hamburg.

[32] Chambers, J., Hollmuller, P., Bouvard, O., Schueler, A., Scartezzini, J.-L., Azar, E. and Patel, M. K., 2019. Evaluating the electricity saving potential of electrochromic glazing for cooling and lighting at the scale of the non-residential national building stock using a Monte Carlo model. Energy. 185, 136–147. https://doi.org/10.1016/j.energy.2019.07.037.

[33] Sarbu, I and Adam, M., 2014. Experimental and numerical investigations of the energy efficiency of conventional air conditioning systems in cooling mode and comfort assurance in office buildings. Energy and Buildings. 85, 45–58. ISSN 0378-7788, https://doi.org/10.1016/j.enbuild.2014.09.022.

[34] European Commission, Directorate-General for Energy, Pezzutto, S., Novelli, A., Zambito, A., 2022. Cooling technologies overview and market shares. Part 1 of the study "Renewable cooling under the revised Renewable Energy Directive ENER/C1/2018-493", Publications Office of the European Union. https://data.europa.eu/doi/10.2833/799633.

[35] Kiran Naik, B. and Muthukumar, P., 2017. Empirical Correlation Based Models for Estimation of Air Cooled and Water Cooled Condenser's Performance. Energy Procedia. 109, 293–305. 10.1016/j.egypro.2017.03.070.

[36] Albawi, S., Mohammed, T. A. and Al-Zawi, S., 2017. Understanding of a convolutional neural network. 2017 International Conference on Engineering and Technology (ICET), pp. 1–6. DOI: 10.1109/ICEngTechnol.2017.8308186.

[37] Liu, L., Ouyang, W., Wang, X., Fieguth, P., Chen, J., Liu, X. and Pietikäinen, M., 2020. Deep Learning for Generic Object Detection: A Survey. International Journal of Computer Vision. 128, 261–318. https://doi.org/10.1007/s11263-019-01247-4.

[38] Zhao, Z.-Q., Zheng, P., Xu, S.-t. and Wu, X., 2019. Object Detection With Deep Learning: A Review. IEEE Transactions on Neural Networks and Learning Systems. 30(11), 3212–3232. DOI: 10.1109/TNNLS.2018.2876865.

[39] Nguyen, N.-D., Do, T., Ngo, T. D. and Le, D.-D., 2020. An Evaluation of Deep Learning methods for Small Objects Detection. Journal of Electrical and Computer Engineering. 2020. https://doi.org/10.1155/2020/3189691.

[40] Zou, Z., Shi, Z., Gou, Y. and Ye, J., 2019. Object detection in 20 Years: A Survey. Computer Vision and Pattern Recognition. https://arxiv.org/abs/1905.05055v2.

[41] LeCun, Y., Bengio, Y. Hinton, G., 2015. Deep learning. Nature. 521, 436–444. https://doi.org/10.1038/nature14539.

[42] Groener, A., Chern, G. and Pritt, M., 2019. Comparison of Deep Learning Object Detection Models for Satellite Imagery. 2019 IEEE Applied Imagery Pattern Recognition Workshop (AIPR), Washington, DC, USA, 2019, pp. 1–10. DOI: 10.1109/AIPR47015.2019.9174593.

[43] Guo, W., Yang, W., Zhang, H. and Hua, G., 2018. Geospatial Object Detection in High Resolution Satellite Images Based on Multi-Scale Convolutional Neural Network. Remote Sensing. 10, 131. https://doi.org/10.3390/rs10010131.

[44] Haroon, M., Shahzad, M. and Fraz, M.M., 2020. Multisized Object Detection Using Spaceborne Optical Imagery. IEEE Journal of Selected Topics in Applied Earth Observations and Remote Sensing. 13, 3032–3046.

[45] Mansour, A., Hassan, A., Hussein, W. M. and Said, E., 2019. Automated vehicle detection in satellite images using deep learning. IOP Conference Series: Materials Science and Engineering. 610 012027.

[46] Niesser, R., Schilling, H., Hinz, S. and Jutzi, B., 2018. Klassifikation von Fahrzeugen aus RGB und LiDAR-Daten mit Convolutional Neural Networks. 38. Wissenschaftlich-Technische Jahrestagung der DGPF und PFGK18 Tagung, München, 7-9. März 2018. Hrsg.: T.P. Kersten. DGPF. ISSN: 0942-2870.

[47] Pang, J., Li, C., Shi, J., Xu, Z. and Feng, H., 2019. R2-CNN: Fast Tiny Object Detection in Large-Scale Remote Sensing Images. Computer Vision and Pattern Recognition. DOI: 10.1109/TGRS.2019.2899955.

[48] Wagh, P., Das, D. and Damani, O.P., 2019. Well Detection in Satellite Images using Convolutional Neural Networks. Conference: 5th International Conference on Geographical Information Systems Theory, Applications and Management. DOI: 10.5220/0007734901170125.

[49] Towerscout, 2021. https://groups.ischool.berkeley.edu/TowerScout/ (accessed 02.12.2021).

[50] Tan, M., Pang, R. and Le, Q. V., 2020. EfficientDet: Scalable and Efficient Object Detection. 2020 IEEE/CVF Conference on Computer Vision and Pattern Recognition (CVPR), Seattle, WA, USA, 2020, pp. 10778–10787, DOI: 10.1109/CVPR42600.2020.01079. arXiv:1911.09070.

[51] Roboflow, 2022. Product Overview. https://roboflow.com/ (accessed 27.04.2022).

[52] Ramachandran, P., Zoph, B. and Le, Q.V., 2017. Searching for Activation Functions. Neural and Evolutionary Computing. arXiv:1710.05941v2.

[53] Zhang, X., 2011. Regularization, in: Sammut, C. and Webb, G.I., 2011. Encyclopedia of Machine Learning. Springer. Boston, MA. DOI: https://doi.org/10.1007/978-0-387-30164-8_712.

[54] Adnot, J., Riviere, P., Marchio, D., Holmstrom, M., Naeslund, J., Saba, J., Becirspahic, S., Lopes, C., Blanco, I., Perez-Lombard, L., Ortiz, J., Papakonstantinou, N., Doukas, P., Joppolo, C. M., Casale, C., Benke, G., Giraud, D., Houdant, N., Colomines, F., Gavriliuc, R., … Hitchin, R., 2003. Energy Efficiency and Certification of Central Air Conditioners (EECCAC). Final Report – April 2003.

[55] Berger, H. and Eisenhut, T., 2012. Energieffiziente Kühlsysteme. Beispiele für effiziente industrielle Kühlung. Endbericht. Report Rep-0376. ISBN 978-3-99004-179-6.

[56] Aquaprox, 2007. Kühlwasserbehandlung. Berlin Heidelberg: Springer, 2007. ISBN 978-3-540-71098-1.

[57] Hall, S., 2012. 10 - Cooling Towers, in: Brenan's Rules of Thumb for Chemical Engineers (Fifth Edition). Butterworth-Heinemann, pp. 182–189. ISBN 9780123877857.

[58] Everingham, M. and Winn, J., 2012. The PASCAL Visual Object Classes Challenge 2012 (VOC2012) Development Kit. http://host.robots.ox.ac.uk/pascal/VOC/voc2012/devkit_doc.pdf.

[59] Cartucho, J., Ventura, R. and Veloso, M., 2018. Robust Object Recognition Through Symbiotic Deep Learning In Mobile Robots. 2018 IEEE/RSJ International Conference on Intelligent Robots and Systems (IROS). pp. 2336–2341.

[60] Ting, K.M., 2011. Confusion Matrix, in: Sammut, C. and Webb, G.I., 2011. Encyclopedia of Machine Learning. Springer. Boston, MA. DOI: https://doi.org/10.1007/978-0-387-30164-8_712.

[61] Sammut, C. and Webb, G.I., 2011. F1-Measure. Encyclopedia of Machine Learning. Springer. Boston, MA. DOI: https://doi.org/10.1007/978-0-387-30164-8_712.

[62] Schiewer, H.-J., s.a. Uni'umweltbericht 2018/2019. Albert-Ludwigs-Universität Freiburg. Hofmann Druck, Emmendingen.

[63] Pan-European Thermal Atlas 5.2, 2022. https://www.arcgis.com/apps/webappviewer/index.html?id=8d51f3708ea54fb9b732ba0c94409133 (accessed: 07.03.2022).

[64] He, K., Gkioxari, G., Dollár, P. and Girshick, R., 2018. Mask R-CNN. Computer Vision and Pattern Recognition. arXiv:1703.06870.

Appendix

Table A. 1. Overview for the created training, calibration and evaluation data sets for the detection of condensers of air-cooled chillers (ACCs) and cooling towers (CTs) and the estimation of the cooling capacity corresponding to the workflow (Fig. 1 b & c).

Task			Criteria	Training data	Evaluation data
b)	Object detection		Location	3000 images (5553 ACCs, 3204 CTs)	147 images (335 ACCs, 145 CTs, 46 blank images)
c)	Quantification of cooling capacities	ACC Evaluation	Number of fans	366 images (244 ACCs, 2066 Fans)	51 images (335 ACCs)
		CT Calibration	Fan size	50 images (211 CTs)	-
		CT Evaluation	Fan size	-	50 images (145 CTs)